Mismatch-Induced Conformational Distortions in Polymerase β Support an Induced-Fit Mechanism for Fidelity†

Karunesh Arora,‡ William A. Beard,§ Samuel H. Wilson,§ and Tamar Schlick*,‡

Department of Chemistry and Courant Institute of Mathematical Sciences, New York University, 251 Mercer Street, New York, New York 10012, and Laboratory of Structural Biology, National Institute of Environmental Health Sciences, National Institutes of Health, P.O. Box 12233, Research Triangle Park, North Carolina 27709-2233

Received April 27, 2005; Revised Manuscript Received June 24, 2005

ABSTRACT: Molecular dynamics simulations of DNA polymerase (pol) β complexed with different incorrect incoming nucleotides (G·G, G·T, and T·T template base·incoming nucleotide combinations) at the template−primer terminus are analyzed to delineate structure−function relationships for aberrant base pairs in a polymerase active site. Comparisons, made to pol β structure and motions in the presence of a correct base pair, are designed to gain atomically detailed insights into the process of nucleotide selection and discrimination. In the presence of an incorrect incoming nucleotide, α-helix N of the thumb subdomain believed to be required for pol β's catalytic cycling moves toward the open conformation rather than the closed conformation as observed for the correct base pair (G·C) before the chemical reaction. Correspondingly, active-site residues in the microenvironment of the incoming base are in intermediate conformations for non-Watson−Crick pairs. The incorrect incoming nucleotide and the corresponding template residue assume distorted conformations and do not form Watson−Crick bonds. Furthermore, the coordination number and the arrangement of ligands observed around the catalytic and nucleotide binding magnesium ions are mismatch specific. Significantly, the crucial nucleotidyl transferase reaction distance (P_α−O3′) for the mismatches between the incoming nucleotide and the primer terminus is not ideally compatible with the chemical reaction of primer extension that follows these conformational changes. Moreover, the extent of active-site distortion can be related to experimentally determined rates of nucleotide misincorporation and to the overall energy barrier associated with polymerase activity. Together, our studies provide structure−function insights into the DNA polymerase-induced constraints (i.e., α-helix N conformation, DNA base pair bonding, conformation of protein residues in the vicinity of dNTP, and magnesium ions coordination) during nucleotide discrimination and pol β−nucleotide interactions specific to each mispair and how they may regulate fidelity. They also lend further support to our recent hypothesis that additional conformational energy barriers are involved following nucleotide binding but prior to the chemical reaction.

DNA polymerases play a key role in maintaining genome integrity (*1*−*3*). Eukaryotic DNA polymerase β (pol β)[1] is a DNA repair enzyme that preferentially selects the correct nucleotide (e.g., C opposite G) instead of an incorrect unit (e.g., A opposite G) during DNA repair and replication synthesis. Experimental data suggest an "induced-fit" mechanism (*4*, *5*) between the DNA-bound polymerase and substrate: the correct substrate aligns catalytic groups as required for proper synthesis ("fidelity"), while an incorrect unit distorts the geometric and electrostatic environment so that DNA synthesis is hampered. The fidelity of DNA polymerases broadly refers to their ability to incorporate correct rather than incorrect nucleotides complementary to the template DNA (*6*); such fidelities span a wide range, from one to nearly 10^6 errors per 1 million nucleotides incorporated. DNA pol β is a moderate fidelity polymerase belonging to the X-family of DNA polymerases; it fills short DNA gaps during base excision repair and has an average base substitution error frequency of one per 10^3 bases synthesized (*7*, *8*).

The fidelity of DNA polymerases in selecting the correct dNTP is attributed to several structural factors: Watson−Crick hydrogen bonding (*9*, *10*), the steric fit between the incoming dNTP and the polymerase active-site pocket (including template) (*11*), and the pattern of hydrogen bonding between polymerases and duplex DNA bases (*12*). Although Watson−Crick hydrogen bonding plays a significant role in pairing selectivity and stabilizing the existing DNA helix, steric and geometric aspects of the active site are believed to play an important role in maintaining DNA synthesis fidelity (*10*, *13*, *14*).

† This work was supported by NSF Grant ASC-9318159, NIH Grants R01 GM55164 and R01 ES012692, Intramural Research Program of the NIH, and National Institute of Environmental Health Sciences. Acknowledgment is also made to the donors of the American Chemical Society Petroleum Research Fund for support (or partial support) of this research (Award PRF39115-AC4 to T.S.).

* To whom correspondence should be addressed. Phone: (212) 998-3116. E-mail: schlick@nyu.edu. Fax: (212) 995-4152.

‡ New York University.

§ National Institutes of Health.

[1] Abbreviations: pol β, DNA polymerase β; dNTP, 2′-deoxyribonucleoside 5′-triphosphate; ddCTP, 2′,3′-dideoxyribocytidine 5′-triphosphate; dCTP, 2′-deoxyribocytidine 5′-triphosphate; MD, molecular dynamics.

10.1021/bi0507682 CCC: $30.25
Published on Web 09/15/2005

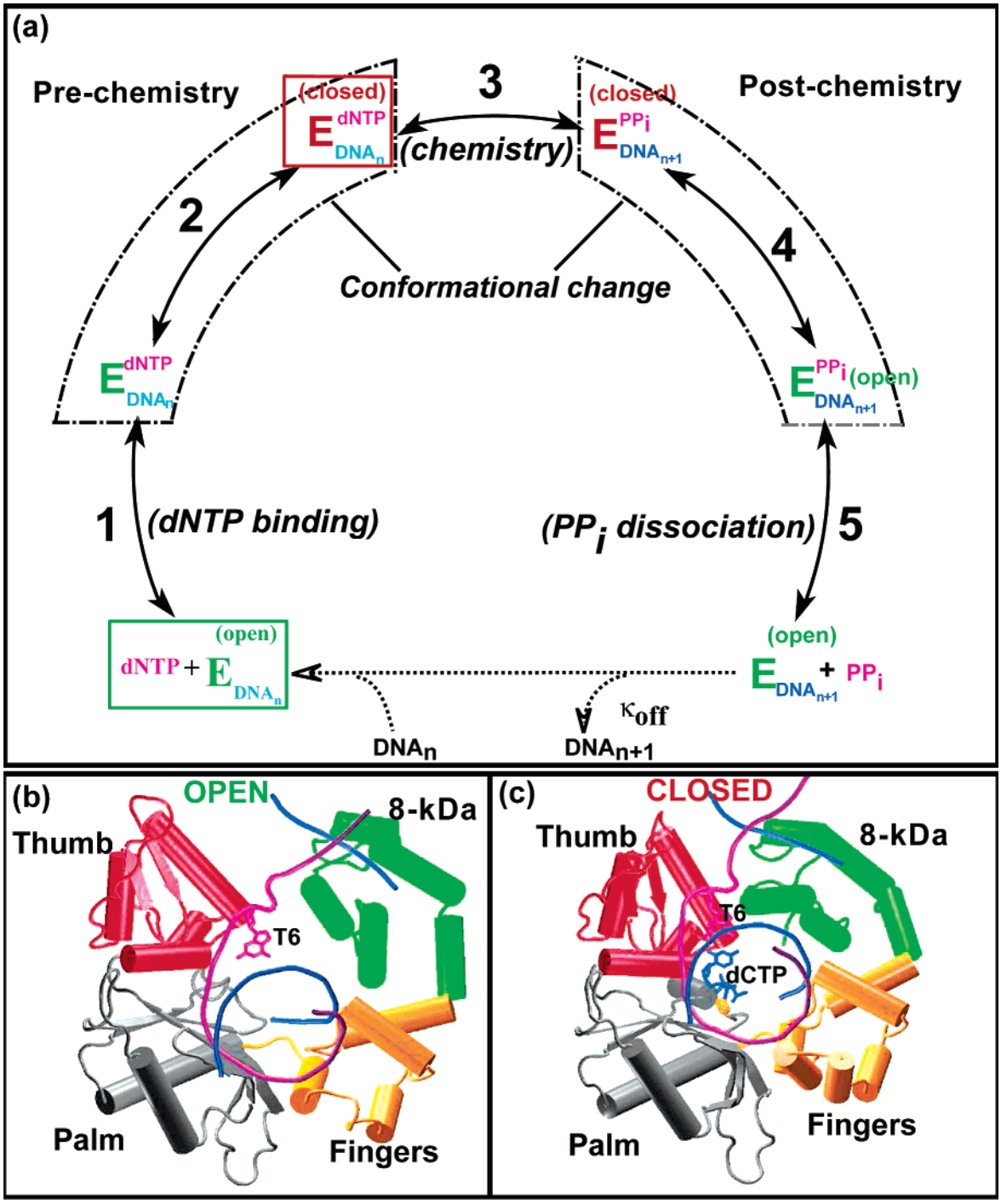

FIGURE 1: (a) General pathway for nucleotide insertion by pol β and corresponding crystal open (b) and closed (c) conformations of the pol β−DNA complex. E represents DNA polymerase, dNTP 2′-deoxyribonucleoside 5′-triphosphate, PP_i pyrophosphate, and DNA_n/DNA_{n+1} DNA before/after nucleotide incorporation to DNA primer. T6 is a template residue (G) for the incoming nucleotide (dCTP).

Structurally, pol β is composed of only two domains, an amino-terminal 8 kDa region which exhibits deoxyribose-phosphate lyase activity and a 31 kDa carboxyl-terminal domain which possesses nucleotidyl transfer activity. The 31 kDa domain shares an overall handlike architecture similar to that of other structurally characterized DNA polymerases, containing finger, palm, and thumb subdomains (*15*). Pol β is "left-handed", while polymerases from other families are "right-handed". Pol β lacks an intrinsic 3′ to 5′ proofreading activity.

Three crystallographic structures representing the polymerase reaction pathway (see Figure 1) have been obtained for pol β (*5*): open binary complex, containing pol β bound to a DNA substrate with a single nucleotide gap; closed ternary complex, containing pol β·gap·ddCTP [pol β bound to gapped DNA as well as 2′,3′-dideoxyribocytidine 5′-triphosphate (ddCTP)]; and open binary product complex (pol β·nick), pol β bound to nicked DNA. Panels b and c of Figure 1 illustrate the significant conformational difference (∼7 Å in the thumb subdomain) between these open and closed forms. Recently, DNA pol β structures with mismatches (A·C and T·C, denoting template·primer units in the nascent base pair binding pocket) were also determined (*16*). The structure of the mispairs indicates that α-helix N

is in an "intermediate" conformation and the bases of the mispair do not form hydrogen bonds with one another.

On the basis of kinetic and structural studies of various DNA polymerases (*17*−*30*), a common nucleotide insertion pathway has been deduced in which the enzyme undergoes transitions between open and closed forms (Figure 1a). At step 1, following DNA binding, the DNA polymerase binds a 2′-deoxyribonucleoside 5′-triphosphate (dNTP) to form an open substrate complex; this complex is assumed to undergo a conformational change to align catalytic groups and form a closed ternary complex at step 2; the nucleotidyl transferase reaction then follows. The 3′-OH of the primer strand attacks P_α of the incoming dNTP to extend the primer strand and form the ternary product complex (step 3); this complex then undergoes conformational changes (step 4) leading to the open enzyme form. This transition is followed by dissociation of pyrophosphate (PP_i) (step 5), after which the DNA synthesis−repair cycle can begin anew.

The conformational rearrangements involved in steps 2 and 4 are believed to be key for monitoring DNA synthesis fidelity (*5*). Binding of the correct nucleotide is thought to induce the first conformational change (step 2), whereas binding of an incorrect nucleotide may alter or inhibit the conformational transition. This "induced-fit" mechanism was thus proposed to explain the polymerase fidelity in the selection of the correct dNTP (*5*). This mechanism suggests that the conformational changes triggered by binding of the correct nucleotide will align the catalytic groups as needed for catalysis, whereas the incorrect substrate will somehow interfere with this process. However, no direct experiments have shown this effectively. It is only recently that the structures of pol β bound to a mispair (*16*, *47*), along with those for high-fidelity *Bacillus* DNA polymerase I (*31*) and lesion-bypass polymerase Dpo4 (*32*), have begun to shed new light on the distortions and disruptions within and around the active site of a polymerase when a mismatch is encountered.

Earlier, molecular dynamics simulations of the pol β−DNA complex with the enzyme's active site occupied by either the correct incoming base pair or no substrate have delineated structural and dynamical changes that occur during conformational changes before the nucleotide transferase reaction (*33*). We observed contrasting global subdomain motions as well as alignment of catalytic residues in the presence versus absence of substrate in the pol β binding site. These studies provided in silico support for the substrate-induced conformational change in pol β.

To further explore the induced-fit hypothesis and understand pol β's nucleotide discrimination mechanism, we examine here, by several atomistic molecular dynamics simulations, the structural changes and polymerase−substrate interactions with mismatched base pairs in the polymerase active site. This work complements prior simulations of pol β with mispairs after the nucleotide incorporation (*34*), which helped in the interpretation of kinetic data for DNA mispair extension. This study investigates mispair geometry and flexibility before nucleotide incorporation and helps in the interpretation of kinetic data for pol β nucleotide misinsertion (*19*, *30*, *35*). This investigation is warranted since limited structural information for complexes of DNA polymerases bound to mismatches exists (*16*, *31*, *32*, *48*). Modeling and simulation, combined with available structural information, can help probe such structure−flexibility−function relationships systematically. Because nucleotide incorporation by pol β is a dynamic process, molecular dynamics investigations (*36*−*39*) can provide important snapshots that link and extend experimental structural anchors.

Our dynamics simulations reveal a large thumb subdomain conformational change, closing in the presence of the correct base pair but opening in the presence of mismatched base pairs, consistent with the induced-fit hypothesis. The geometry of each mispair complex at the end of simulations indicates that incoming nucleotides and the corresponding template residue do not form Watson−Crick hydrogen bonds. The magnesium ion coordination and active-site geometries crucial for subsequent catalysis are severely distorted for all mispairs. Furthermore, the coordination number and the arrangement of ligands observed around the catalytic and nucleotide binding magnesium ions are mismatch specific. Significantly, the nucleotidyl transferase reaction distance (P_α−O3′) between the incoming nucleotide and the primer terminus is not ideal for the chemical reaction following the conformational change process. The extent of distortion of the active-site geometry can be qualitatively related to the experimentally determined rates of misincorporation of different mismatches in the pol β active site (*35*). These observations combined with information available from experiments suggest a direct relation between active-site structural distortions and the fidelity of pol β. They also lend further credence to our recent hypothesis that additional conformational energy barriers are involved following nucleotide binding but prior to the chemical reaction.

COMPUTATIONAL METHODOLOGY

Initial Models. All simulations of pol β−DNA complexes with an incorrect incoming nucleotide were started from the intermediate ("half-closed") conformation before the nucleotidyl transferase reaction to capture pol β's closing within 10 ns. This follows our prior experience where the intermediate structure of pol β was successful in capturing the polymerase opening (after the chemical reaction of nucleotidyl transfer) (*36*) and closing (*33*) in the polymerase kinetic cycle. The intermediate forms used in our studies also resemble a crystal intermediate (*16*) and are found on the closing pathway delineated by the stochastic path approach (*38*).

In earlier work, we investigated conformational changes in the pol β−DNA complex in the presence of a correct base pair (G·C) (*33*). There the intermediate model was constructed as an average of the crystallographic open, binary gapped complex (PDB entry 1BPX) and the closed, ternary complex (PDB entry 1BPY) from the RCSB Protein Data Bank (*40*). Specifically, the model's thumb subdomain is partially closed, with the correct base pair (G·C) in the active site. On the basis of this model, complexes of pol β with G·T, G·G, and T·T mispairs (template·incoming dNTP) were built by replacing the correct incoming nucleotide (dCTP) with incorrect nucleotides dTTP, dGTP, and dTTP, respectively. For the T·T mispair, the template G was replaced with T. The protein residues and other DNA base sequences remain unchanged. Both the incoming nucleotide and template are in an anti conformation for all mispairs, following the crystal structure of pol β with a mispair (*16*).

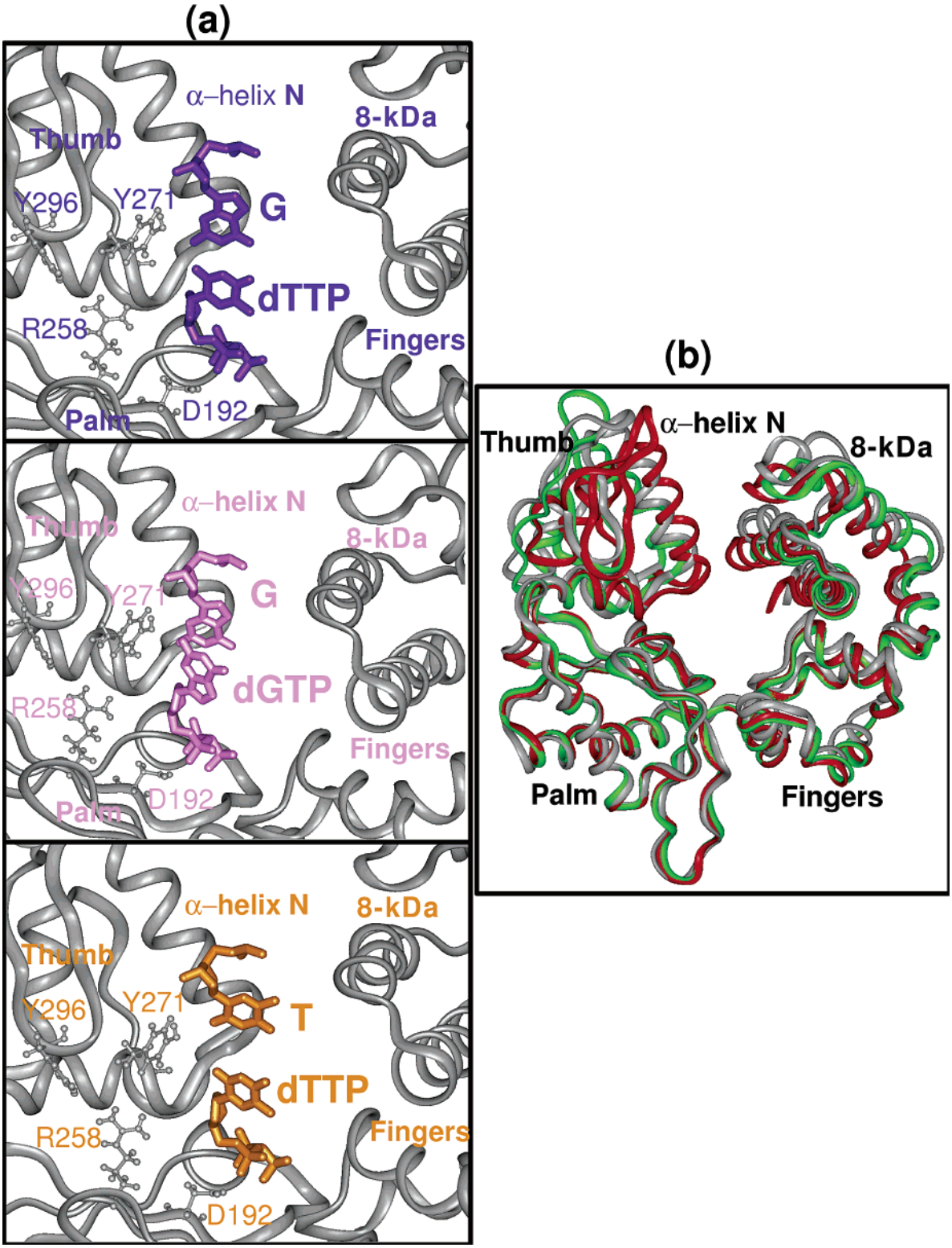

FIGURE 2: (a) Starting structures of G·T (purple), G·G (pink), and T·T (orange) mispairs in the pol β active site. The incoming nucleotides are in the anti conformation in all mispairs. (b) Comparison of one of the initial constructed intermediate models (gray) with respect to the crystallographic binary open (green) and ternary closed structures (red). The conformation of protein in all initial mismatch models is similar. Structures are superimposed with respect to the palm C_α subdomain atoms.

The starting conformations of all three mispairs in the active site are shown in Figure 2a. G·T and T·T mispairs are hydrogen bonded with one another in the initial models. The thumb subdomain is in the intermediate conformation between the crystal "open" and "closed" complex (see Figure 2b).

All mismatch models were similarly solvated in cubic periodic domains using PBCAID (*41*). To neutralize the system at an ionic strength of 150 mM, water molecules (TIP3 model) with minimal electrostatic potential at the oxygen atoms were replaced with Na^+, and those with maximal electrostatic potential were replaced with Cl^-. All

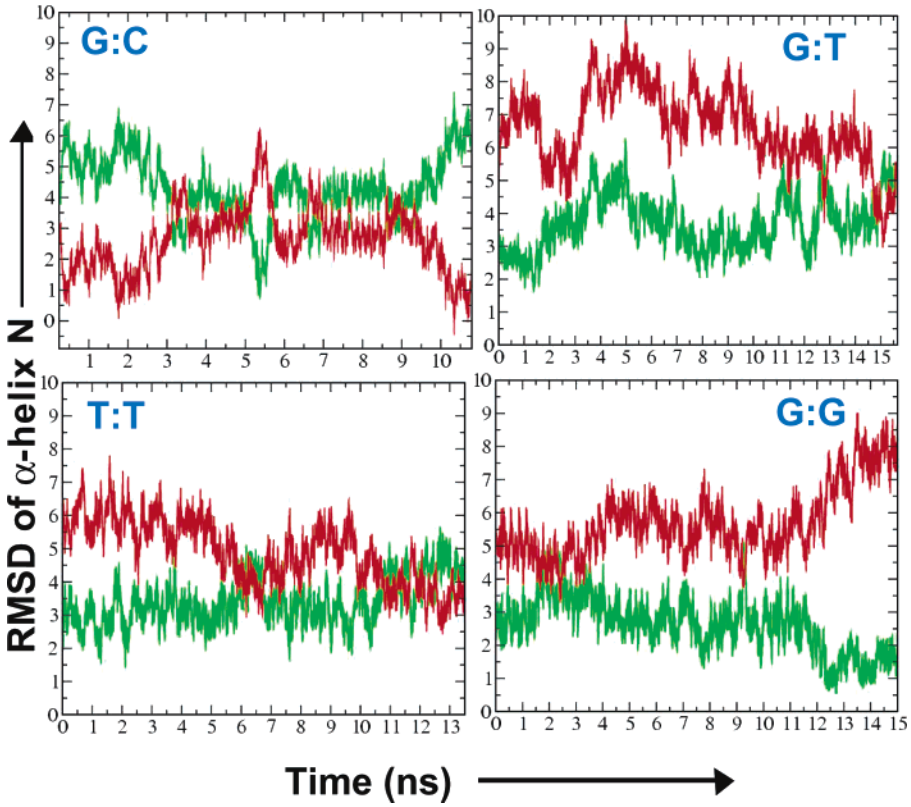

FIGURE 3: Time evolution of the rmsd of α-helix N C_α atoms in all trajectories (G·C, G·T, T·T, and G·G) relative to those in the crystal open (green) and closed (red) structures. All systems are superimposed with the palm subdomain (residues 152−258) C_α atoms.

Na^+ and Cl^- ions were placed more than 8 Å from any protein or DNA atom and from each other. The electrostatic potential for all bulk oxygen atoms was calculated using the DelPhi package (*42*). All solvated systems with mismatch incoming nucleotides contain approximately 40 000 atoms, including water of solvation (11 249 water molecules).

Minimization, Equilibration, and Dynamics Protocol. Energy minimizations, equilibrations, and dynamics simulations for all systems were performed using CHARMM (Chemistry Department, Harvard University, Cambridge, MA) (*43*) with the all-atom version C26a2 force field (*44*). First, each system was minimized with fixed positions of all protein and DNA heavy atoms using steepest descent (SD) for 10 000 steps; this was followed by adapted basis Newton−Raphson minimization (*43*, *45*) for 20 000 steps. The 30 ps of equilibration at 300 K was followed by further minimization using SD and ABNR until the gradient of root-mean-square deviations was less than 10^{-6} kcal mol^{-1} $Å^{-1}$. Finally, the protein/DNA/counterions/water coordinates were re-equilibrated for 30 ps at 300 K by the Langevin multiple-time step method LN [see ref *36* for a thorough examination of the stability and reliability of the integrator for large macromolecular systems in terms of thermodynamic, structural, and dynamic properties compared to single-time step Langevin as well as Newtonian (Velocity Verlet) propagators]. Our triple-time step protocol uses an inner time step $\Delta\tau$ of 1 fs for updating local bonded interactions, a medium time step Δt_m of 2 fs to update nonbonded interactions within 7 Å, and an outer time step Δt of 150 fs for calculating the remaining terms; this yields an acceleration factor of 4 over single-time step Langevin dynamics when $\Delta\tau = 1$ fs. The SHAKE algorithm was employed to constrain the bonds involving hydrogen atoms. Electrostatic and van der Waals interactions were smoothed to zero at 12 Å with a shift function and a switch function, respectively. The Langevin collision parameter (γ) of 10 ps^{-1} was chosen to couple the system to a 300 K heat bath. The total simulation length for each system is between 10 and 15 ns.

RESULTS AND DISCUSSION

Subdomain Conformation and Catalytic Activation. For all mismatch trajectories, started from the intermediate position of α-helix N of the thumb subdomain, we capture movements toward the open conformation observed in the binary pol β structure with gapped DNA (Figure 3). The extent of α-helix N opening is mispair-dependent (see Figure 4). Specifically, the rmsd of α-helix N with respect to the open conformation can be ranked as follows: G·G < T·T < G·T < G·C. Thus, the purine·purine mismatch (G·G) favors the inactive conformation most strongly, while the purine·pyrimidine and pyrimidine·pyrimidine mismatches (G·T and T·T) tend to intermediate conformations between closed and open states as recently observed in the determined crystal mismatch structures (A·C and T·C) of pol β (*16*). A distorted open conformation that differs from that seen in the presence of a cognate base pair was also observed in high-fidelity *Bacillus* DNA polymerase I (*31*); note that there mispairs are at different parts of the catalytic cycle compared to those studied here. In contrast to the open form of the thumb preferred for all mismatch complexes, thumb closing is observed in the presence of the correct nucleotide (G·C). Prior works using dynamics and advanced sampling techniques have shown that thumb closing in the presence of a correct base pair occurs in multiple steps rather than a single concerted manner (*37*, *38*). That is, a metastable conformation exists for the thumb corresponding to a "half-rotated"

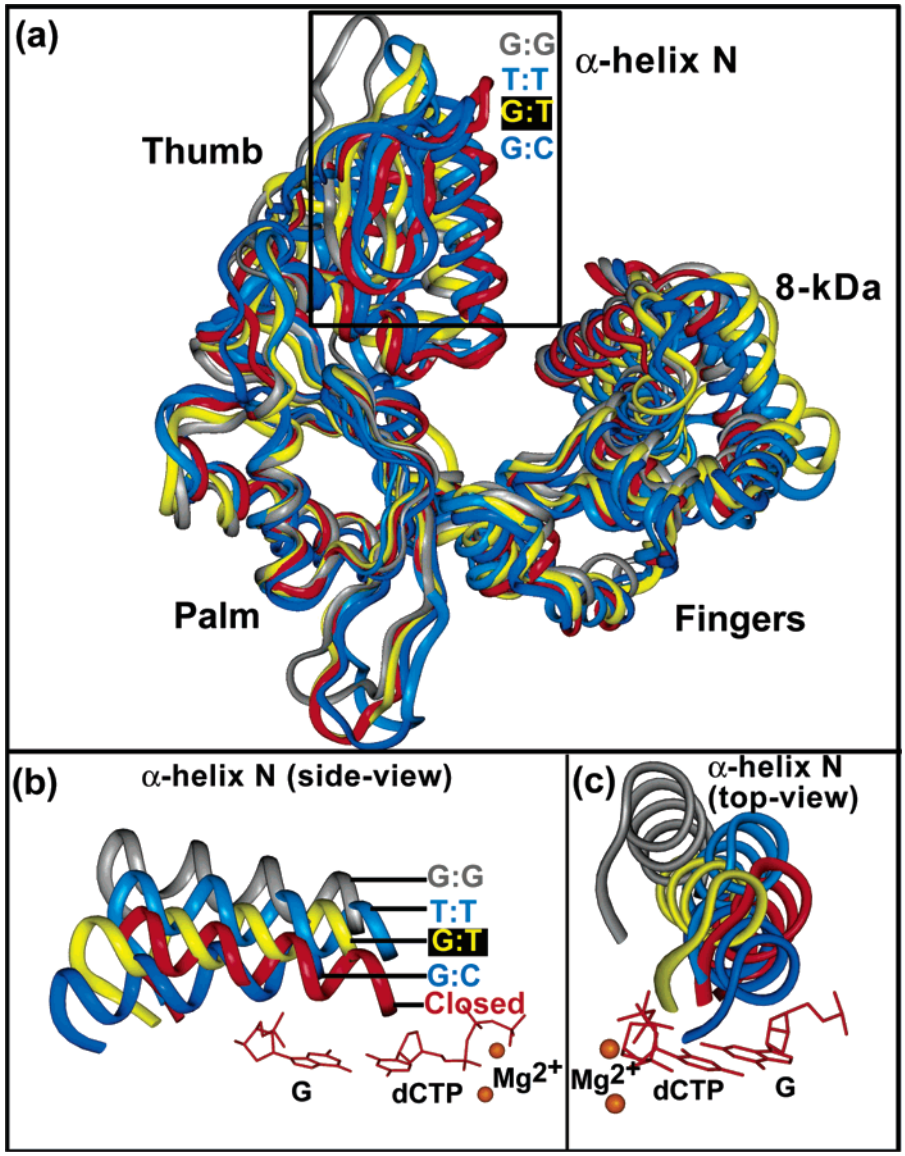

FIGURE 4: Comparison of the simulated systems with the closed crystal structure for (a) the entire pol β and (b and c) α-helix N in the thumb subdomain in two orientations. All systems are superimposed with respect to palm C_α atoms. The colored ribbons identify the closed (red) crystal structure (PDB entry 1BPY) and the simulated G·T (yellow), G·G (gray), T·T (turquoise), and G·C (blue) mismatches.

state of Arg258 on the pathway between crystal open and closed conformations; this thumb movement triggers several side chain motions in the microenvironment of the incoming substrate. In concert, coupled motions produce unique interactions between the polymerase and the substrate present in neither the open nor the closed crystal forms and provide specific suitability checks for pol β to differentiate correct from incorrect substrates. We speculate that a disruption of the thumb closing in the presence of a mismatched incoming nucleotide might signal a stalling of such a reaction pathway. The observed global thumb conformational changes in response to mismatched incoming substrates are consistent with the proposed induced-fit mechanism for DNA polymerase fidelity.

More specifically, from structural analyses of pol β in the crystal open and closed conformations, several key residues (Asp192, Phe272, and Arg258) have been implicated to act in concert with the thumb's movement (*5*). In the open thumb conformation, Asp192 is engaged in a salt bridge with Arg258, while in the closed thumb conformation, the phenyl ring of Phe272 disrupts the salt bridge between Asp192 and Arg258, freeing Asp192 to ligate both active-site metal ions. The closed conformation also puts the side chains of thumb residue Tyr296 in position to hydrogen bond with Arg258, ensuring that Arg258 will not interfere with Asp192's ability to ligate the metal ion. According to the current induced-fit hypothesis, the conformational closing (in the presence of a correct nucleotide) prepares these residues in the binding site for the subsequent step of nucleotidyl transfer along the polymerase kinetic pathway (Figure 1).

Figure 5 shows the conformation of these key active-site residues in the presence of correct versus incorrect incoming nucleotides as observed during the simulations. For the correct incoming nucleotide (dCTP), Asp192 coordinates both magnesium ions and Phe272 insulates Asp192 from Arg258 by intervening between these side chains. In the G·T mismatch conformations, these residues are positioned like those in the presence of the correct incoming nucleotide. For G·G and T·T, Asp192 coordinates the magnesium ions but Phe272 is not positioned between Asp192 and Arg258 and instead resembles the conformation of Phe272 in the open

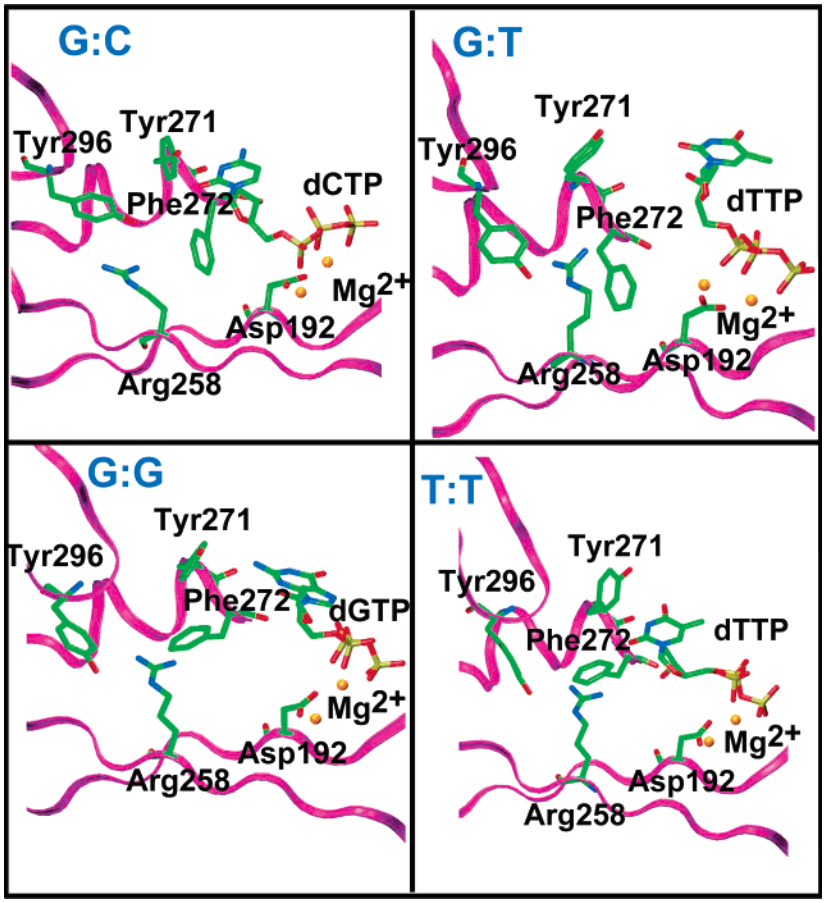

FIGURE 5: Conformation of key active-site residues in the simulated pol β−DNA complexes with different incoming nucleotides as observed during last 1 ns of G·C, G·T, G·G, and T·T trajectories.

thumb conformation. Figure 6 depicts the conformation of Phe272 in all trajectories as characterized by two dihedral angles. To determine the position of Arg258 during the simulations, we follow in Figure 7 the interatomic distance evolutions of Arg258 NH1 with respect to both Asp192 OD1 and Tyr296 OH in the presence of correct and incorrect nucleotides. The figure shows how Arg258 rotates and forms a hydrogen bond with Tyr296 in the matched (G·C) and mismatched (G·T) trajectories. However, for the G·G and T·T mismatch simulations, distances between Arg258 and Tyr296 remain constant throughout the trajectory as in the starting intermediate conformation. Thus, results indicate that the motion of key active-site residues (Arg258, Asp192, and Tyr296) is correlated with the thumb subdomain movement (see Figure 4), which in turn is related to the presence and the type of the incoming nucleotide in the base pair binding pocket.

The thumb subdomain movement toward open or closed states can also be interpreted by following the motion of protein residues Asp276, Arg283, Asn279, and Lys280 that interact with the nascent base pair only in the closed conformation.

Structural and kinetic analyses of pol β mutants involving residues at the active site suggest that the selection of the incoming nucleotide is guided by the templating residue via an induced-fit mechanism (*46*). The templating residue is not properly aligned to base pair with the incoming nucleotide in the open thumb conformation, but thumb closure favors the active conformation of the template by directly forming van der Waals contacts with the template, anchoring it to the polymerase (*5*).

In Figure 8, we follow the evolution of distances between the nascent base pair binding residues (Asp276, Arg283, Asn279, and Lys280) and the DNA template base in the presence of correct and incorrect nucleotides. Figure 8 (top left) shows that template binding residues move to interact with the DNA template G in the presence of the correct incoming nucleotide. In the G·T mismatch simulation as illustrated in Figure 8 (top right), the templating residues first move away from the DNA template but then move toward it as the trajectory evolves. For the G·G and T·T mismatch simulations where the thumb assumes the open conformation, the templating residues evolve away from the template (Figure 8, bottom). The observed motion of the templating residues is also directly correlated with the thumb's conformational change.

Nascent Base Pair Conformation in the DNA Pol β Active Site. In Figure 9, we superimpose the nascent base pair and two neighboring primer−template DNA base pairs in the simulated G·C, G·T, G·G, and T·T systems with corresponding base pairs in the closed crystal ternary pol β DNA complex with correct incoming nucleotide according to the protein C_α atoms. The DNA base pairs in the closed crystal pol β DNA complex serve as a reference in determining the distortion of the nascent base pairs in the matched and mismatched structures. The simulated correct base pair deviates slightly from the perfect Watson−Crick pairing, but the deviations are much greater for incorrect incoming

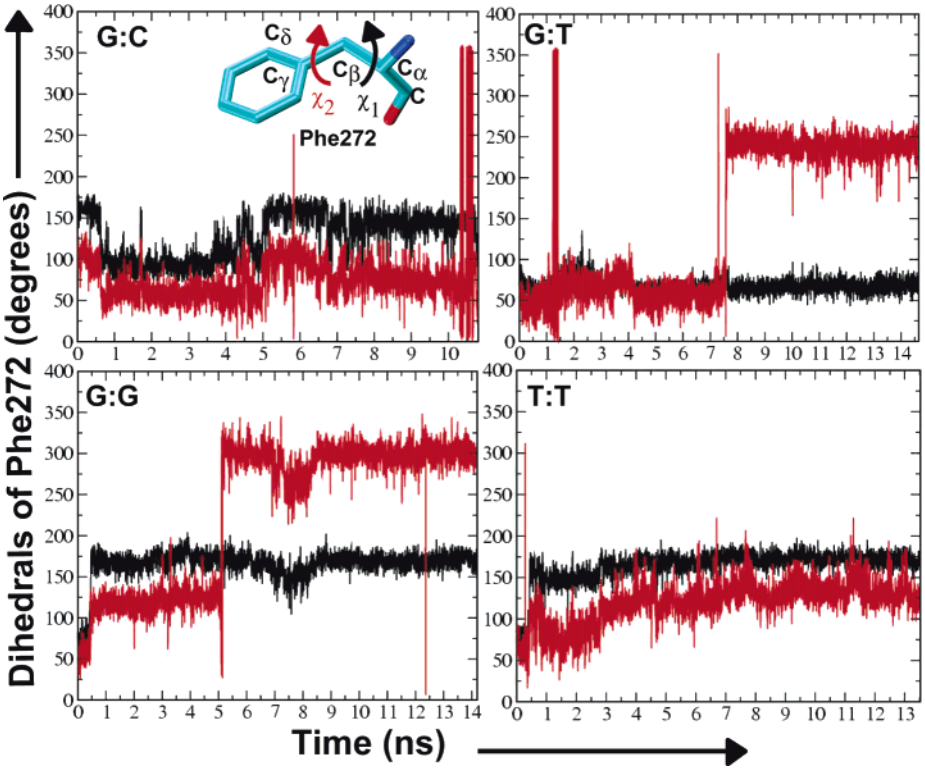

FIGURE 6: Time evolution of dihedral angles associated with the Phe272 phenyl ring over the trajectories. The two dihedral angles of Phe272 are defined by the following atomic sequence: χ_1 for C−C_α−C_β−C_γ and χ_2 for C_α−C_β−C_γ−C_δ. In the crystal open conformation (PDB entry 1BPX), dihedral angles χ_1 and χ_2 are 146° and 167°, respectively; in the crystal closed conformation (PDB entry 1BPY) χ_1 and χ_2 correspond to 96° and 21°, respectively.

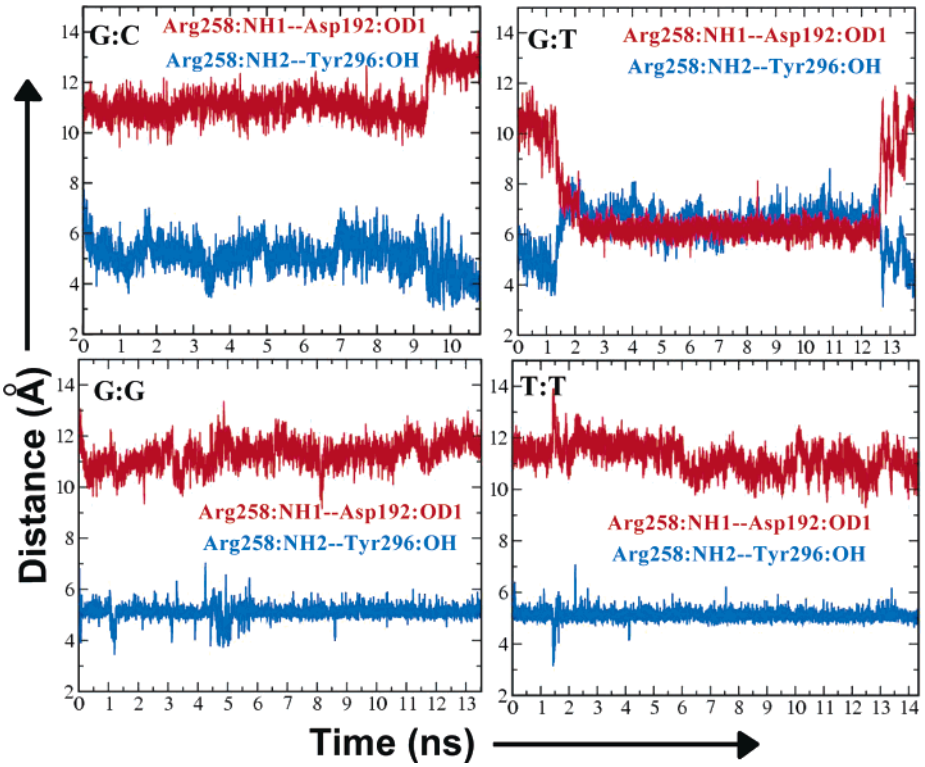

FIGURE 7: Time evolution of atom−atom distances for Arg283 NH1 with both Asp192 OD1 and Tyr296 OH in the mismatched trajectories.

nucleotides. Interestingly, for all mispair geometries, either the primer or template strand slides toward the major groove (see Figure 9). Template bases G and T are displaced toward the major groove in the G·T and T·T mispairs, respectively. For the G·G and G·T mispairs, the incoming nucleotide bases are displaced toward the major groove. The template and primer bases slide toward the major groove to varying degrees relative to the corresponding base pair in the crystal closed complex. Displacement of the incoming nucleotide distances of the α-phosphorus from the primer terminus results in a longer P_α−O3′ distance and discourages incorrect nucleotide insertion.

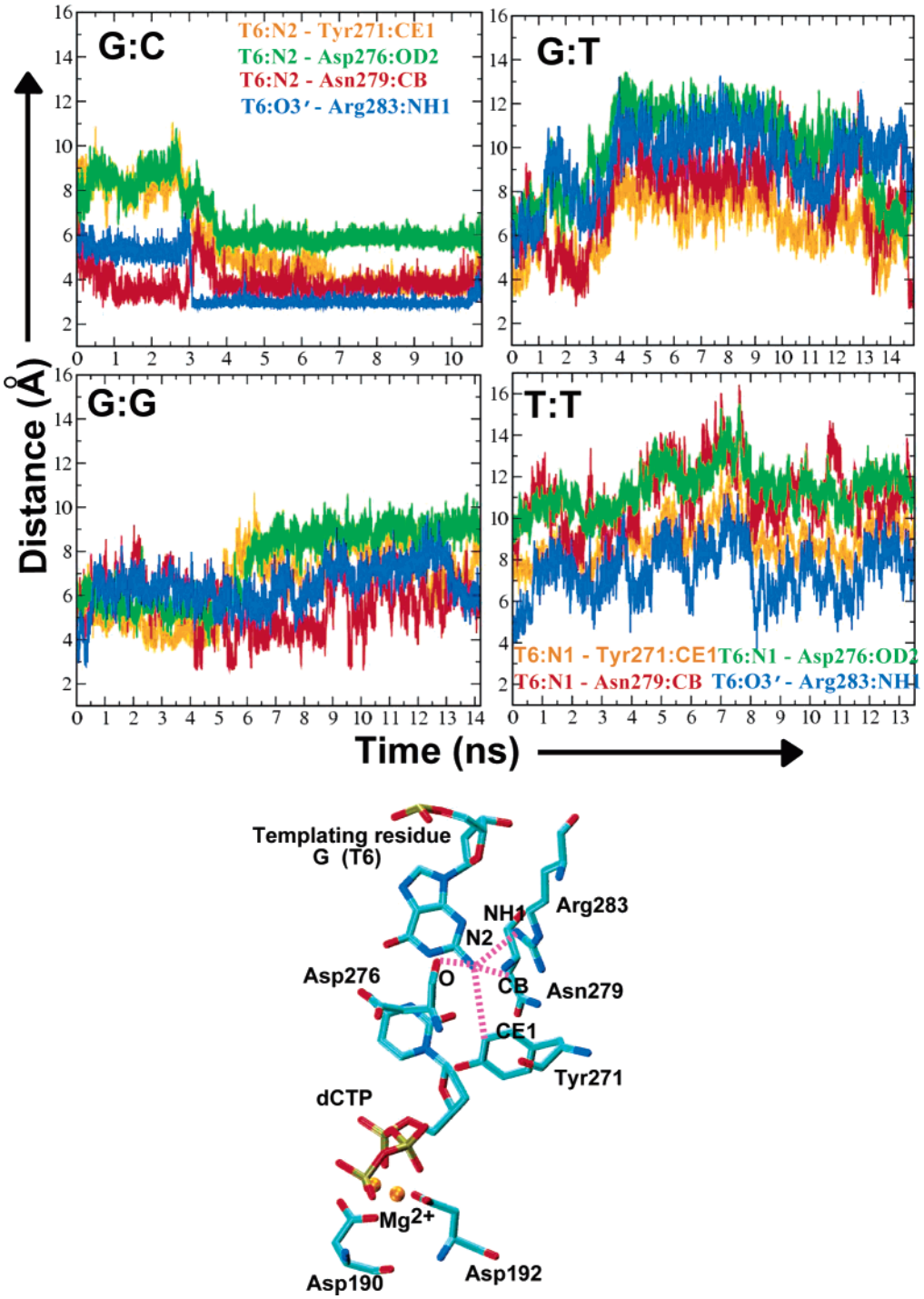

FIGURE 8: Time evolution of distances between the nascent base pair and protein residues Asp276, Asn279, and Arg283 in all mismatched trajectories. Distances for the correct base pair (G·C) are diagrammed (below) with dashed lines.

We also note non-Watson−Crick interactions within all mispairs; in particular, the base pairs stack against one another in the G·G mispair. This staggered conformation of nascent base pairs in the confines of the pol β active site is consistent with the structure of a purine·purine mismatch in the pol β active site (*47*).

According to the geometric selection model, steric size and shape complementarity of nascent base pairs are more crucial than the ability to form Watson−Crick hydrogen bonds (*9*, *10*). The ability of several DNA polymerases to insert nonpolar nucleoside isosteres that do not form Watson−Crick bonds is consistent with this model (*48*, *49*). Still, the significance of Watson−Crick hydrogen bonding in determining DNA polymerase synthesis and high fidelity appears to be polymerase-dependent (*50*). For example, pol β fails to replicate nonpolar isosteres, indicating that minor groove hydrogen bonds with the template base and incoming nucleotide may be crucial in the nucleotide selection process.

Our prior work investigated three mismatched base pairs, namely, G·G, A·C, and C·C (template·primer) mismatches at the DNA polymerase active site after chemistry (step 4 in Figure 1) (*34*). It appeared that the hierarchy of distortions for these base pairs (G·G > C·C > A·C) paralleled the experimentally determined ability of pol β to extend these mispairs. The work here investigates mispairs, namely, G·G, G·T, and T·T (template·incoming nucleotide) mismatches

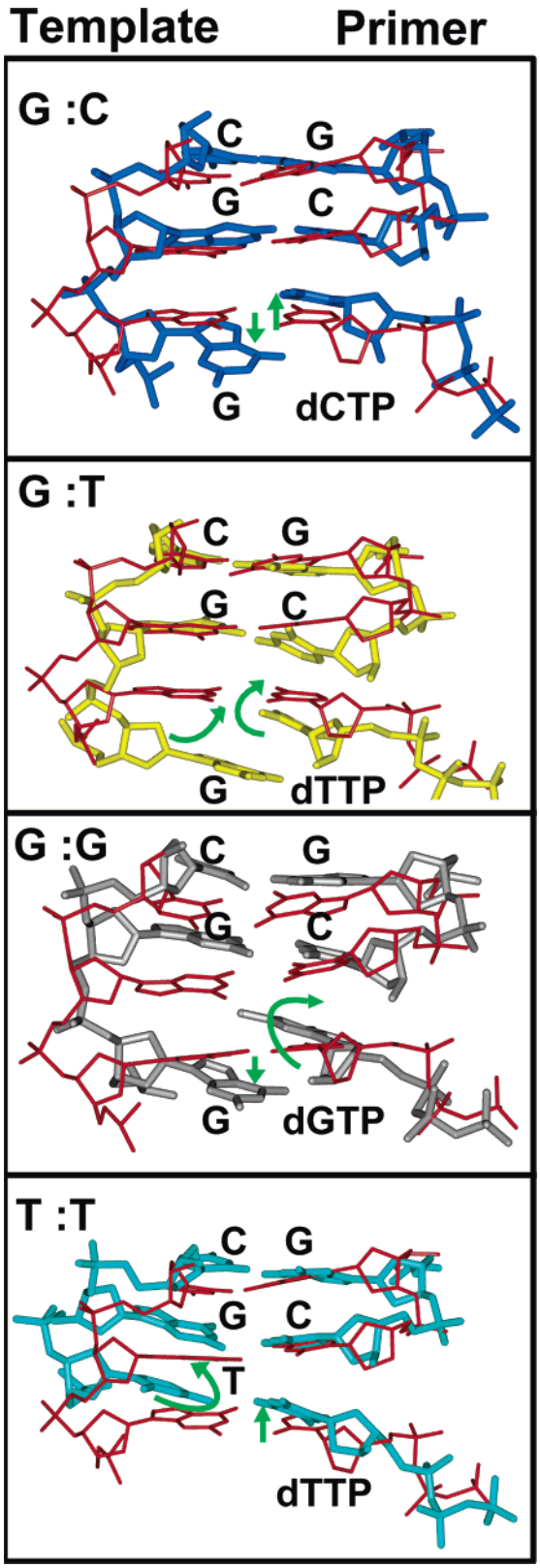

FIGURE 9: Conformational comparisons of active-site base pairs and two neighboring base pairs in the crystal closed (red) vs simulated G·C (blue), G·T (yellow), G·G (gray), and T·T (cyan) pol β−DNA complexes. The nascent base pair plane in the closed crystal complex (red) is used for reference. Structures are superimposed using C_α atoms of protein residues 10−335 of pol β. The DNA minor groove is nearest the viewer, whereas the major groove is farthest from the viewer. The arrows (green) depict the deviation from the Watson−Crick bonding. The labels on DNA bases correspond to the simulated structures.

at the polymerase active site before the nucleotide incorporation (step 2 in Figure 1). The observed mispair distortions in pol β in either case, before or after nucleotidyl transferase reaction, are quite similar. That is, Watson−Crick pairing is not observed for the mispairs, and in general, purine·purine (e.g., G·G) mismatches are most severely distorted and difficult to incorporate or extend. Kinetic analyses of the incorporation and extension of all 12 mispairs by pol β agree with the trends observed in our simulations (*35*).

Mismatch-Induced Disruption of the Active-Site Geometry. DNA polymerase structures are consistent with a "two-metal-ion" mechanism (*51*−*53*) of nucleotide incorporation: the incoming nucleotide is accompanied by a magnesium ion (the nucleotide binding ion) that coordinates the phosphoryl oxygen atoms with all three phosphate groups. In addition, a catalytic magnesium ion coordinates a phosphoryl oxygen atom of the α-phosphate group. In pol β, these magnesium ions are coordinated in the active site by oxygen atoms of three conserved aspartate residues (Asp190, Asp192, and Asp256). According to this two-metal-ion mechanism, the catalytic Mg^{2+} lowers the affinity of the proton in the primer 3′-OH group, facilitating the 3′-O attack on the P_α of the incoming nucleotide (*54*, *55*). The nucleotide-binding Mg^{2+} assists the pyrophosphate's departure, and both ions stabilize the structure of the presumed pentacoordinated transition state. However, in the available crystal ternary pol β−DNA complex with a correct incoming nucleotide, the primer terminus lacks the 3′-OH group. The recently reported crystal structures of DNA mismatches (template·primer, A·C and T·C) in the active site were determined by using nicked product DNA that traps the mispair in the nascent base pair binding pocket (*16*). Thus, the effect of the missing 3′-OH on the magnesium ion coordination and the pol β active-site geometry cannot be inferred from the available structural information.

In our simulations, we modeled the missing 3′-OH group at the primer terminus in all starting structures. Figure 10 shows the coordination of both catalytic and nucleotide binding magnesium ions as observed during the simulations for matched versus mismatched incoming nucleotides at the template−primer terminus. Clearly, the ligand arrangement around both magnesium ions is mispair specific. Already, the magnesium ion coordination sphere for the correct base pair differs from that observed in the ternary closed crystal complex of pol β; in the crystal structure (PDB entry 1BPY) (*5*), the catalytic magnesium ion is found coordinated with the cation bound to OD2 of Asp256, nonbridging O1A of the substrate (dCTP), OD1 of Asp192, and the carboxylate oxygen atoms of Asp190. In addition, a water molecule was postulated to coordinate with catalytic magnesium, though this is not observed in the electron density map (*5*). Interestingly, this predicted water molecule becomes bound to the catalytic ion during the simulation in the presence of the correct incoming nucleotide (*33*) and is observed in a high-resolution (1.65 Å) structure of pol β ternary complex recently determined in the Wilson lab (unpublished results). Some differences in ligand coordination are listed in Table 1 and have been discussed previously (*33*), where we identify nonideal geometries as an indication that an additional high-energy barrier must be surmounted before chemical reaction (see further discussion at end of this subsection). Most strikingly, we note larger than expected distances between

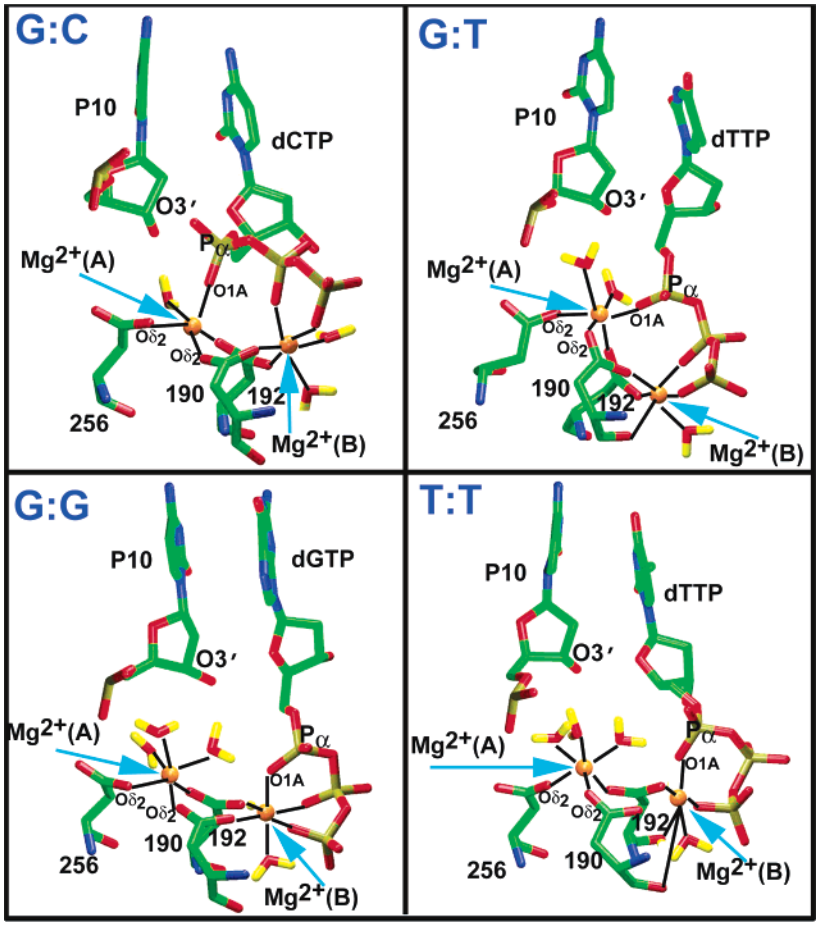

FIGURE 10: Catalytic [Mg^{2+} (A)] and nucleotide [Mg^{2+} (B)] binding magnesium ion coordination environment reflected at the end of G·C, G·T, G·G, and T·T trajectories. Black lines are drawn to the coordinated oxygen atoms. Average distances over the final 1 ns for atoms coordinating the magnesium ions are listed in Table 1.

Table 1: Average Active-Site Interatomic Distances for the Simulated Matched (G·C) and Mismatched (G·T, G·G, and T·T) Simulations[a]

	distance (Å)				
	G·C[b]	G·T	G·G	T·T	G·C[c] crystal
nucleotidyl transfer distance					
dNTP (P_α)−P10 (O3′)	4.19	4.11	4.97	5.53	n/a[d]
catalytic magensium ion coordination					
Mg^{2+}(A)−P10 (O3′)	4.98	4.51	4.36	4.41	n/a[d]
Mg^{2+}(A)−dNTP (O1A)	1.81	1.89	4.26	4.26	2.37
Mg^{2+}(A)−256 (Oδ2)	1.81	1.87	1.83	1.83	2.60
Mg^{2+}(A)−192 (Oδ1)	1.83	1.84	1.86	1.85	2.20
nucleotide magnesium ion coordination					
Mg^{2+}(B)−dNTP (O1A)	4.06	3.78	1.93	1.93	1.94
Mg^{2+}(B)−192 (Oδ2)	1.86	1.84	1.85	1.87	1.97
Mg^{2+}(B)−dNTP (O2γ)	1.81	1.89	1.83	1.83	2.00
Mg^{2+}(A)−Mg^{2+}(B)	4.07	4.26	4.38	4.37	3.37

[a] Mg^{2+}(A), catalytic magnesium; Mg^{2+}(B), nucleotide binding magnesium; dNTP, 2′-deoxynucleoside 5′-triphosphate; P10, primer terminus. [b] Template, incoming nucleotide. [c] PDB entry 1BPY. [d] Not available.

the catalytic magnesium ion and the modeled O3′, not present in the crystal structure; the O3′ atom is expected to coordinate the catalytic ion to complete the coordination sphere. In addition, the O1A atom on the α-phosphorus of the incoming nucleotide coordinates only one of the magnesium ion and not both ions, as also suggested by the closed ternary crystal complex (PDB entry 1BPY).

For the mismatched incoming substrates in the active site, magnesium ion coordination departs further from the perfect ligand arrangement as assumed to be required for the subsequent nucleotidyl transferase reaction (see Figure 10 and Table 1). Though the magnesium ions are hexacoordinated, ligands that complete the coordination are distinct for each mispair and also depart from that for the correct pair. This implies loss of other interactions with protein side chains and the incoming nucleotide triphosphate, leading to more water molecules coordinating the catalytic magnesium ion which completes the ion coordination sphere in all mispair active-site geometries. According to Petruska et al. (*56*), enzymes amplify free energy differences between the correct and incorrect base pair by partially excluding water from the active site, thus increasing enthalpy differences and reducing entropy differences and leading to improved fidelity. Water exclusion and enthalpy−entropy compensation has been put forward as a likely explanation for the fidelity of polymerases being higher than that which can be explained by free energy differences between correct and incorrect base pairs in aqueous solution.

The coordination of the magnesium ions directly influences the nucleotidyl transferase reaction that follows subdomain motion. Presumably, this chemical reaction occurs by means of either a metal-assisted (Mg^{2+} ion) dissociative mechansim or associative in-line nucleophilic attack on P_α of the incoming nucleotide by 3′-OH of the DNA primer terminus, producing an extended DNA primer. The ideal P_α−O3′

Table 2: Base Substitution Fidelity of Pol β Taken from refs *19* and *35*

enzyme complex	rate constant[a] k_{pol} (s^{-1})	fidelity[b]	catalytic efficiency k_{pol}/K_d (M^{-1} s^{-1})
G−dCTP	10	n/a[c]	750000
G−dTTP	0.0058	63560	12
G−dGTP	0.00029	2885000	0.3
T−dTTP	0.00032	1533000	0.5

[a] Rate constant k_{pol} is the rate of nucleotide incorporation for first-enzyme turnover. [b] Fidelity = error frequency^{-1} = $[(k_{pol}/K_d)_c + (k_{pol}/K_d)_i]/(k_{pol}/K_d)$, where c and i denote correct and incorrect nucleotide incorporation, respectively, and K_d (micromolar) is the apparent equilibrium dissociation constant of dNTP. [c] Not available.

distance for the phosphoryl transferase reaction to proceed via a dissociative mechanism should be around 3.3 Å (*57*). In our simulations, we observe that the crucial P_α−O3′ distance is larger than the ideal distance in the presence of both correct and incorrect incoming nucleotides in the pol β active site. For incorrect compared to correct incoming nucleotides, the P_α−O3′ distance is greater by 1−2 Å. These notable deviations from the ideal active-site geometries compatible with nucleotidyl transferase reactions imply a hampering of the incorrect nucleotide incorporation permitting the incorrect dNTP to diffuse away.

On the basis of the discussion presented above, we propose that the extent of distortion of pol β's active-site geometry can be broadly described by three crucial distances [P_α−O3′, catalytic Mg^{2+}−O3′, and catalytic Mg^{2+}−dNTP (O1A)] required to be within ideal distance for the chemical reaction of nucleotidyl transfer. With these distance criteria, the hierarchy of the mismatch-induced distortions of the active-site geometry, in increasing order, is as follows: G·T < G·G ∼ T·T (see Table 2).

On the basis of the experimentally determined kinetic parameters, k_{pol} and K_d, listed in Table 2, the fidelity of different mismatches in pol β can be arranged in the following increasing order: G·T < G·G ∼ T·T. Since fidelity is inversely related to the error frequency, we can infer that the G·T mispair is the most favorable mispair for pol β followed by the G·G and T·T mispairs; the T·T mispair is the least favorable mispair to be misincorporated (*35*). Thus, the degree of active-site geometry distortion determined from our simulations approximately parallels the experimentally determined efficiences of misincorporation for different mismatches. This suggests that a relationship between active-site structural distortion and fidelity may be appropriate for understanding pol β. Moreover, given that most DNA polymerases insert incorrect nucleotides with similar efficiencies (*58*), strategies utilized by pol β to discriminate against incorrect nucleotide may be generally applicable.

This comparative analysis of mispair conformations provides new insights into polymerase mechanisms for the following reasons. Systematic QM/MM investigations of pol β in which active-site atoms treated with the ab initio approach also resulted in larger than expected active-site distances (*59*). Larger distances also arose in dynamics simulations of Dpo4 from the Broyde lab (*60*): 2.5 ns simulations from the ternary complex of Dpo4 with modified/unmodified template and different incoming substrates produced in all but one simulation P_α−O3′ distances far from ideal and larger for mismatches (*60*; Supporting Information Figure S5); though these findings are not discussed in their work, perturbed active-site geometries by another group employing AMBER rather than CHARMM lend credence to our interpretation that these distortions are not mere force field artifacts and that requisite rearrangements before chemistry may have important biological ramifications.

Specifically, this scenario suggests that additional active-site rearrangements must follow the thumb's conformational change so that the system evolves to a state compatible for the chemical reaction. Such conformational changes will likely involve slow and stochastic adjustments of Mg^{2+} and phosphoryl coordination at the pol β active site in a part of the reaction profile we call the "prechemistry avenue" (after subdomain closing but before chemistry). From emerging studies, we speculate that the chemical reaction might proceed from partially open states or suboptimal "activated" complexes for mismatched incoming nucleotides, after these prechemistry avenue changes. The existence of such prechemistry changes is supported by the recently determined A·C and T·C mismatch crystal structures of pol β where the thumb is in an intermediate conformation (*16*). The prechemistry avenue can be viewed as another fidelity check point en route to the chemical reaction that promotes selectivity and hence fidelity. The existence of prechemistry changes does not diminish the role of large subdomain rearrangements, still required, but not rate-limiting, for incoming nucleotide recognition (*19*, *36*, *61*). NMR data from the London and Wilson (*62*) and Mildvan (*63*) groups also suggest localized motions proximal to metal-binding ligands and near the β/γ-phosphates of the incoming nucleotide prior to chemistry but following dNTP binding.

CONCLUDING REMARKS

Our dynamics simulations of pol β−DNA complexes with nascent G·G, T·T, and G·T mispairs before chemistry suggest several structural and dynamic features for all mispairs which may represent mechanisms employed by pol β to evade error initiation. The closing motion of α-helix N of the thumb subdomain required for catalytic cycling of pol β is disrupted in the presence of mispairs in the pol β active site. The extent of thumb opening in trajectories started from an intermediate conformation is mismatch specific. These global conformational changes are consistent with the induced-fit mechanism for substrate discrimination enhancing polymerase fidelity. The induced-fit mechanism can alter enzyme specificity even if conformational changes are not kinetically rate-limiting if nucleotide incorporation involves nonidentical interactions with the active site in a substrate-dependent transition state (*64*).

Besides large-scale conformational motions, there are several subtle local conformational changes in pol β's active site in response to an incoming nucleotide. The specific structural changes are dependent on the identity of the incoming nucleotide. The magnesium ions which are crucial for stabilizing pol β's active site (in the presumed pentacoordinated transition state for the phosphoryl transferase reaction) have distorted ligand arrangements. The extent of distortion of pol β's active-site geometry can be broadly described by three crucial distances [P_α−O3′, catalytic Mg^{2+}−O3′, and catalytic Mg^{2+}−dNTP (O1A)] required to be within ideal distance for the nucleotide transferase

reaction. The degree of active-site geometry distortion determined from our simulations roughly parallels the experimentally determined rates of misincorporation for different mismatches, suggesting a direct relation between active-site structural distortions and fidelity of pol β.

The related chemical reaction distance ($P_\alpha-O3'$) between the matched or mismatched incoming nucleotide and the primer terminus is larger than expected for phosphoryl transfer by a dissociative mechanism (*54*, *65*, *66*). The base of the incorrect nucleotide and its template partner stack against each other rather than forming Watson−Crick hydrogen bonds. Overall, our observed active-site geometries for both the Watson−Crick G·C pair and the mispairs do not exhibit the ideal geometry for the chemical reaction. This suggests that additional subtle adjustments in the pol β active site are required for the system to evolve to the transition state poised for chemistry. The nature of these adjustments, their energetic costs, and the relation to the overall reaction barriers will be the subject of future investigations.

ACKNOWLEDGMENT

Molecular images were generated using VMD (*67*) and the INSIGHTII package (Accelrys Inc., San Diego, CA).

NOTE ADDED IN PROOF

In connection with our delineation here of the subtle conformational changes that occur prior to correct nucleotide insertion and corresponding different pathways for mismatched systems, we would like to clarify the relation of these events to the overall reaction pathway in light of a recent study (*68*). While our data suggest that a micro-event (partial rotation of Arg258) during thumb closing is rate-limiting for thumb closure, we describe here how subsequent important conformational changes occur prior to chemistry. As highlighted in our paper, these "pre-chemistry" events include changes in the coordination sphere of catalytic magnesium which includes O3′ of the primer terminus. Clearly, subtle fine-tuning of active-site atoms will impact chemistry critically. Whether these additional conformational changes should be considered as part of a single step, chemistry, or as discrete steps will ultimately depend on their energetic contribution to catalysis. Indeed, crystallographic and computational methods have helped identify numerous conformational changes involved in polymerase pathways to complement fluorescence data, which may not resolve these aspects. Thus, there is no contradiction between transient-state fluorescence studies by Bakhtina et al. (*68*) and our computational studies (*36*, *37*).

REFERENCES

1. Iwanaga, A., Ouchida, M., Miyazaki, K., Hori, K., and Mukai, T. (1999) Functional mutation of DNA polymerase β found in human gastric cancer: Inability of the base excision repair in vitro, *Mutat. Res. 435*, 121−128.
2. Hoeijmakers, J. H. J. (2001) Genome maintenance mechanisms for preventing cancer, *Nature 411*, 366−374.
3. Starcevic, D., Dalal, S., and Sweasy, J. B. (2004) Is there a link between DNA polymerase β and cancer? *Cell Cycle 3*, 998−1001.
4. Koshland, D. E. (1994) The key-lock theory and the induced fit theory, *Angew. Chem., Int. Ed. Engl. 33*, 2375−2378.
5. Sawaya, M. R., Parsad, R., Wilson, S. H., Kraut, J., and Pelletier, H. (1997) Crystal structures of human DNA polymerase β complexed with gapped and nicked DNA: Evidence for an induced fit mechanism, *Biochemistry 36*, 11205−11215.
6. Beard, W. A., Shock, D. D., Vande Berg, B. J., and Wilson, S. H. (2002) Efficiency of correct nucleotide insertion governs DNA polymerase fidelity, *J. Biol. Chem. 277*, 47393−47398.
7. Wilson, S. H. (1998) Mammalian base excision repair and DNA polymerase β, *Mutat. Res. 407*, 203−215.
8. Osheroff, W. P., Beard, W. A., Wilson, S. H., and Kunkel, T. A. (1999) Base subsitution specificity of DNA polymerase β depends on interactions in the DNA minor groove, *J. Biol. Chem. 274*, 20749−20752.
9. Watson, J. D., and Crick, F. H. C. (1953) Genetical implications of the structure of deoxyribonucleic acid, *Nature 171*, 964−967.
10. Kool, E. T. (1998) Replication of non-hydrogen bonded bases by DNA polymerases: A mechanism for steric matching, *Biopolymers 48*, 3−17.
11. Echols, H., and Goodman, M. F. (1991) Fidelity mechanism in DNA replication, *Annu. Rev. Biochem. 60*, 477−511.
12. Kunkel, T. A., and Wilson, S. H. (1998) DNA polymerases on the move, *Nat. Struct. Biol. 5*, 95−99.
13. Kool, E. T., Morales, J. C., and Guckian, K. M. (2000) Mimicking the structure and function of DNA: Insight into DNA stability and replication, *Angew. Chem., Int. Ed. 39*, 990−1009.
14. Goodman, M. F. (1997) Hydrogen bonding revisited: Geometric selection as a principal determinant of DNA replication fidelity, *Proc. Natl. Acad. Sci. U.S.A. 94*, 10493−10495.
15. Joyce, C. M., and Steitz, T. A. (1994) Function and structure relationships in DNA polymerases, *Annu. Rev. Biochem. 63*, 777−822.
16. Krahn, J. M., Beard, W. A., and Wilson, S. H. (2004) Structural insights into DNA polymerase β deterrents for misincorporation support an induced-fit mechanism for fidelity, *Structure 12*, 1823−1832.
17. Ahn, J., Werneburg, B. G., and Tsai, M.-D. (1997) DNA polymerase β: Structure-fidelity relationship from pre-steady-state kinetic analyses of all possible correct and incorrect base pairs for wild type and R283A mutant, *Biochemistry 36*, 1100−1107.
18. Ahn, J., Kraynov, V. S., Zhong, X., Werneburg, B. G., and Tsai, M.-D. (1998) DNA polymerase β: Effects of gapped DNA substrates on dNTP specificity, fidelity, processivity and conformational changes, *Biochem. J. 331*, 79−87.
19. Vande Berg, B. J., Beard, W. A., and Wilson, S. H. (2001) DNA structure and aspartate 276 influence nucleotide binding to human DNA polymerase β, *J. Biol. Chem. 276*, 3408−3416.
20. Shah, A. M., Li, S. X., Anderson, K. S., and Sweasy, J. B. (2001) Y265H mutator mutant of DNA polymerase β. Proper teometric alignment is critical for fidelity, *J. Biol. Chem. 276*, 10824−10831.
21. Suo, Z., and Johnson, K. A. (1998) Selective inhibition of HIV-1 reverse transcriptase by an antiviral inhibitor, (*R*)-9-(2-phosphonylmethoxypropyl)adenine, *J. Biol. Chem. 273*, 27250−27258.
22. Kraynov, V. S., Werneburg, B. G., Zhong, X., Lee, H., Ahn, J., and Tsai, M.-D. (1997) DNA polymerase β: Analysis of the contributions of tyrosine-271 and asparagine-279 to substrate specificity and fidelity of DNA replication by pre-steady-state kinetics, *Biochem. J. 323*, 103−111.
23. Zhong, X., Patel, S. S., Werneburg, B. G., and Tsai, M.-D. (1997) DNA polymerase β: Multiple conformational changes in the mechanism of catalysis, *Biochemistry 36*, 11891−11900.
24. Dahlberg, M. E., and Benkovic, S. J. (1991) Kinetic mechanism of DNA polymerase I (Klenow fragment): Identification of a second conformational change and evaluation of the internal equilibrium constant, *Biochemistry 30*, 4835−4843.
25. Kuchta, R. D., Mizrahi, V., Benkovic, P. A., Johnson, K. A., and Benkovic, S. J. (1987) Kinetic mechanism of DNA polymerase I (Klenow), *Biochemistry 26*, 8410−8417.
26. Wong, I., Patel, S. S., and Johnson, K. A. (1991) An induced-fit kinetic mechanism for DNA replication fidelity: Direct measurement by single-turnover kinetics, *Biochemistry 30*, 526−537.
27. Patel, S. S., Wong, I., and Johnson, K. A. (1991) Pre-steady-state kinetic analysis of processive DNA replication inducing complete characterization of an exonuclease-deficient mutant, *Biochemistry 30*, 511−525.
28. Frey, M. W., Sowers, L. C., Millar, D. P., and Benkovic, S. J. (1995) The nucleotide analog 2-aminopurine as a spectroscopic probe of nucleotide incorporation by the Klenow Fragment of *Escherichia coli* polymerase I and bacteriophage T4 DNA polymerase, *Biochemistry 34*, 9185−9192.
29. Capson, T. L., Peliska, J. A., Kaboord, B. F., Frey, M. W., Lively, C., Dahlberg, M., and Kovic, S. J. (1992) Kinetic characterization of the polymerase and exonuclease activities of the gene 43 protein of bacteriophage T4, *Biochemistry 31*, 10984−10994.

30. Beard, W. A., Shock, D. D., Yang, X.-P., DeLauder, S. F., and Wilson, S. H. (2002) Loss of DNA polymerase β stacking interactions with templating purines, but not pyrimidines, alters catalytic efficiency and fidelity, *J. Biol. Chem. 277*, 8235−8242.
31. Johnson, S. J., and Beese, L. S. (2004) Structures of mismatch replication errors observed in a DNA polymerase, *Cell 116*, 803−816.
32. Trincao, J., Johnson, R. E., Wolfle, W. T., Escalante, C. R., Prakash, S., Prakash, L., and Aggarwal, A. K. (2004) Dpo4 is hindered in extending a G•T mismatch by a reverse wobble, *Nat. Struct. Biol. 11*, 457−462.
33. Arora, K., and Schlick, T. (2004) In silico evidence for DNA polymerase β's substrate-induced conformational change, *Biophys. J. 87*, 3088−3099.
34. Yang, L., Beard, W. A., Wilson, S. H., Roux, B., Broyde, S., and Schlick, T. (2002) Local deformations revealed by dynamics simulations of DNA polymerase β with DNA mismatches at the primer terminus, *J. Mol. Biol. 321*, 459−478.
35. Beard, W. A., Shock, D. D., and Wilson, S. H. (2004) Influence of DNA structure on DNA polymerase β active site function: Extension of mutagenic DNA intermediates, *J. Biol. Chem. 279*, 31921−31929.
36. Yang, L., Beard, W. A., Wilson, S. H., Broyde, S., and Schlick, T. (2002) Polymerase β simulations reveal that Arg258 rotation is a slow step rather than large subdomain motion *per se*, *J. Mol. Biol. 317*, 651−671.
37. Radhakrishnan, R., and Schlick, T. (2004) Orchestration of cooperative events in DNA synthesis and repair mechanism unravelled by transition path sampling of DNA polymerase β's closing, *Proc. Natl. Acad. Sci. U.S.A. 101*, 5970−5975.
38. Arora, K., and Schlick, T. (2005) The conformational transition pathway of polymerase β/DNA complex upon binding correct incoming substrate, *J. Phys. Chem. B 109*, 5358−5367.
39. Arora, K., and Schlick, T. (2003) Deoxyadenosine sugar puckering pathway simulated by the stochastic difference equation algorithm, *Chem. Phys. Lett. 378*, 1−8.
40. Berman, H. M., Westbrook, J., Feng, Z., Gilliland, G., Bhat, T. N., Weissig, H., Shindyalov, I. N., and Bourne, P. E. (2000) The protein data bank, *Nucleic Acids Res. 28*, 235−242.
41. Qian, X., Strahs, D., and Schlick, T. (2001) A new program for optimizing periodic boundary models of solvated biomolecules (PBCAID), *J. Comput. Chem. 22*, 1843−1850.
42. Klapper, I., Hagstrom, R., Fine, R., Sharp, K., and Honig, B. (1986) Focusing of electric fields in the active site of Cu−Zn superoxide dismutase: Effects of ion strength and amino-acid modification, *Proteins 1*, 47−59.
43. Brooks, B. R., Bruccoleri, R. E., Olafson, B. D., States, D. J., Swaminathan, S., and Karplus, M. (1983) CHARMM: A program for macromolecular energy, minimization, and dynamics calculations, *J. Comput. Chem. 4*, 187−217.
44. MacKerell, A. D., Jr., and Banavali, N. K. (2000) All-atom empirical force field for nucleic acids: II. Application to molecular dynamics simulations of DNA and RNA in solution, *J. Comput. Chem. 21*, 105−120.
45. Schlick, T. (1992) Optimization methods in computational chemistry, in *Reviews in Computational Chemistry* (Lipkowitz, K. B., and Boyd, D. B., Eds.) Vol. III, pp 1−71, VCH Publishers, New York.
46. Beard, W. A., and Wilson, S. H. (1998) Structural insights into DNA polymerase β fidelity: Hold it tight if you want it right, *Chem. Biol. 5*, R7−R13.
47. Krahn, J. M., Beard, W. A., Miller, H., Grollman, A. P., and Wilson, S. H. (2003) Structure of DNA polymerase β with the mutagenic DNA lesion 8-oxodeoxyguanine reveals structural insights into its coding potential, *Structure 11*, 121−127.
48. Moran, S., Ren, R. X.-F., and Kool, E. T. (1997) A thymidine triphosphate shape analog lacking Watson−Crick paring ability is replicated with high sequence selectivity, *Proc. Natl. Acad. Sci. U.S.A. 94*, 10506−10511.
49. Kool, E. T. (2001) Hydrogen bonding, base stacking, and steric effects in DNA replication, *Annu. Rev. Biophys. Biomol. Struct. 30*, 1−22.
50. Morales, J. C., and Kool, E. T. (2000) Functional hydrogen-bonding map of the minor groove binding tracks of six DNA polymerases, *Biochemistry 39*, 12979−12988.
51. Beese, L. S., and Steitz, T. A. (1991) Structural basis for the 3′-5′ exonuclease activity of *Escherichia coli* DNA polymerase I: A two metal ion mechanism, *EMBO J. 9*, 25−33.
52. Steitz, T. A. (1998) A mechanism for all polymerases, *Nature 391*, 231−232.
53. Bolton, E. C., Mildvan, A. S., and Boeke, J. D. (2002) Inhibition of reverse transcription in vivo by elevated manganese ion concentration, *Mol. Cell 9*, 879−889.
54. Abashkin, Y. G., Erickson, J. W., and Burt, S. K. (2001) Quantum chemical investigation of enzymatic activity in DNA polymerase β. A mechanistic study, *J. Phys. Chem. B 105*, 287−292.
55. Rittenhouse, R. C., Apostoluk, W. K., Miller, J. H., and Straatsma, T. P. (2003) Characterization of the active site of DNA polymerase β by molecular dynamics and quantum chemical calculation, *Proteins: Struct., Funct., Genet. 53*, 667−682.
56. Petruska, J., Goodman, M. F., Boosalis, M. S., Cheong, L. C., and Tinoco, J. I. (1988) Comparison between DNA melting thermodynamics and DNA polymerase fidelity, *Proc. Natl. Acad. Sci. U.S.A. 85*, 6252−6256.
57. Mildvan, A. S. (1997) Mechanisms of signaling and related enzymes, *Proteins: Struct., Funct., Genet. 29*, 401−416.
58. Beard, W. A., and Wilson, S. H. (2003) Structural insights into the origins of DNA polymerase fidelity, *Structure 11*, 489−496.
59. Radhakrishnan, R., and Schlick, T. (2005) Fidelity discrimination in DNA polymerase β (G:A) versus matched (G:C) base pair, *J. Amer. Chem. Soc.*, in press.
60. Perlow-Poehnelt, R. A., Likhterov, I., Scicchitano, D. A., Geacintov, N. E., and Broyde, S. (2004) The spacious active site of a Y-family DNA polymerase facilities promiscuous nucleotide incorporation opposite a bulky carcinogen-DNA adduct, *J. Biol. Chem. 279*, 36951−36961.
61. Arndt, J. W., Gong, W., Zhong, X., Showalter, A. K., Liu, J., Dunlap, C. A., Lin, Z., Paxson, C., Tsai, M.-D., and Chan, M. K. (2001) Insight into the catalytic mechanism of DNA polymerase β: Structures of intermediate complexes, *Biochemistry 40*, 5368−5375.
62. Bose-Basu, B., DeRose, E. F., Kirby, T. W., Mueller, G. A., Beard, W. A., Wilson, S. H., and London, R. E. (2004) Dynamic characterization of a DNA repair enzyme: NMR studies of [*methyl*-^{13}C] methionine-labeled DNA polymerase β, *Biochemistry 43*, 8911−8922.
63. Ferrin, L. J., and Mildvan, A. S. (1986) NMR studies of the conformations and interactions of substrates and ribonucleotide templates bound to the large fragment of DNA polymerase ι, *Biochemistry 25*, 5131−5145.
64. Post, C. B., and Ray, W. J., Jr. (1995) Reexamination of induced fit as a determinant of substrate specificity in enzymatic reactions, *Biochemistry 34*, 15881−15885.
65. Steitz, T. A. (1993) DNA- and RNA-dependent DNA polymerases, *Curr. Opin. Struct. Biol. 3*, 31−38.
66. Lahiri, S. D., Zhang, G., Dunaway-Mariano, D., and Allen, K. N. (2003) The pentacovalent phosphorus intermediate of a phosphoryl transfer reaction, *Science 299*, 2067−2071.
67. Humphrey, W., Dalke, A., and Schulten, K. (1996) VMD-Visual Molecular Dynamics, *J. Mol. Graphics 14*, 33−38.
68. Bakhtina, M., Lee, S., Wang, Y., Dunlap, C., Lamarche, B., and Tsai, M. D. (2005) Use of Viscogens, dNTPaS, and Rhodium (III) as Probes in Stopped-Flow Experiments To Obtain New Evidence for the Mechanism of Catalysis by DNA Polymerase β, *Biochemistry 44*, 5177−5187.

BI0507682